



---

*Research article*

## **Effects of inter-cavity corrosion on metallic wall ties in masonry structures**

**Igor A Chaves\*, Robert E Melchers, Barbara Jardim do Nascimento, Jordan Philips, and Mark Masia**

Centre for Infrastructure Performance and Reliability, The University of Newcastle, Australia

\* **Correspondence:** Email: [igor.chaves@newcastle.edu.au](mailto:igor.chaves@newcastle.edu.au); Tel: +61-02-4921-2006.

**Abstract:** An important structural component for cavity brick and masonry-veneer construction are wall ties. Typically, they are galvanized steel, sufficiently strong to provide continuity for transmission of direct and shear forces. However, field observations show they are prone to long-term corrosion and this can have serious structural implications under extreme events such as earthquakes. Opportunistic observations show corrosion occurs largely to the internal masonry interface zone even though conventional Code requirements specify corrosion testing for the whole tie. To throw light on the issue electrochemical test for 2 grades of galvanized ties and 316 stainless steels combined with three different mortar compositions are reported. Most severe corrosion occurred at the masonry interface and sometimes within the masonry itself. Structural capacity tests showed galvanized ties performed better than stainless steel ties in lieu of stainless steel R4 class ties presenting significantly greater relative losses of yield strength, ultimate tensile strength and elongation structural capacity compared to R2 low galvanized and R3 heavy galvanized tie classes.

**Keywords:** masonry; brick veneer; wall ties; galvanized steel; stainless steel; corrosion

---

### **1. Introduction**

Galvanized mild steel wall ties have long been used in cavity brick and in masonry veneer structures. The ties provide an important degree of structural continuity between masonry leaves in cavity brick construction or between masonry and supporting timber stud or metal stud framing systems [1–4]. By being located in a closed cavity and also being widely spatially distributed within

the masonry wall system for any structure, they are difficult to inspect individually or in cohorts sufficiently large for adequate structural assessments.

Little attention was paid to the condition of wall ties, even in older construction, until it was found, during renovation of 1930s housing in the UK, that the then-used galvanized steel studs showed serious corrosion at the lower ends. This was attributed eventually to the humidity of the cavity space, particularly in older, poorly ventilated forms of cavities in masonry construction [1,3]. The issue of corrosion in the masonry cavity was revealed in earthquake damage of structural masonry [4–6] and in storm damage [7–10] particularly for older structures, in some cases with the outer masonry leaf falling away from the rest of the structure to reveal a multitude of corroded brick ties (Figure 1).

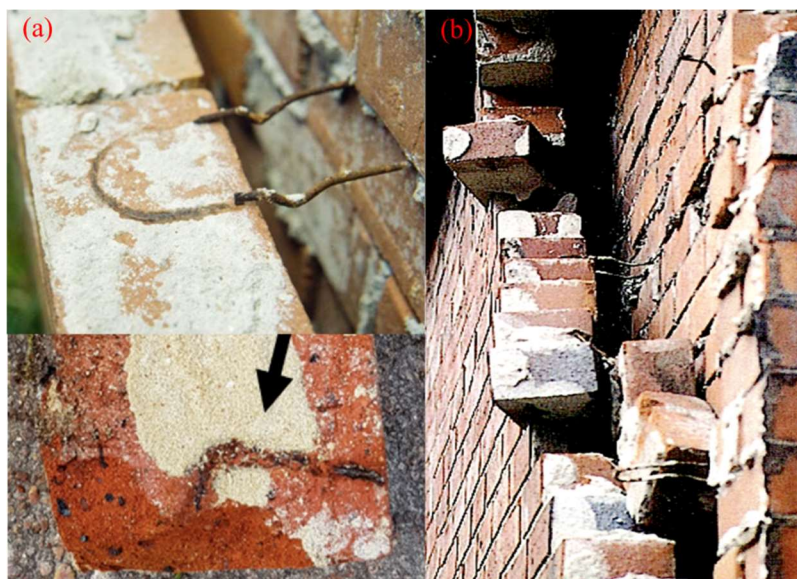


**Figure 1.** (a) Examples of loss of wall-tie connection through corrosion and mortar degradation, and (b) failed cavity brick wall. Note brick dislodgement due to degraded mortar and corroded wall ties.

Efforts to mitigate cavity corrosion of ties have included the increasing use of polymer wall ties. Unfortunately, for structural applications involving high demands for lateral structural stability and capacity, polymer wall ties are unable to provide the required capacity. Increasing use also is being made of heavy-duty galvanized wall ties (galvanized thickness equivalent to  $950 \text{ g/m}^2$  as compared with the conventional galvanized wall ties (typically  $470 \text{ g/m}^2$  or less) [4,7,11,12]. There also has been the introduction of 316 (marine grade) stainless steel for wall ties [11,12], despite their higher cost. These trends apply largely to new or recent construction, even though sufficient understanding of the material failure mechanisms for heavy duty and stainless wall ties remains unresolved [3,4]. In addition, better understanding of the behaviour and corrosion characteristics of conventional (low galvanized) ties remains important since much of the world's older, existing masonry structures are fitted with these types of galvanized wall ties [4,5]. Some of these older structures may be over 50 years old and were constructed well before the introduction of modern design standards, including those for wall ties [3,6]. For these reasons the long-term behaviour and durability of galvanized and stainless-steel wall ties for masonry construction remains of interest. Understanding of such durability and material and structural strength capacity also has serious implications for sustainability of older masonry

structures.

Observations such as those in Figure 1 and other field observations [4,13,14] suggest that the most serious corrosion of conventional wall ties occurs at the interior surface of the outer masonry leaf and sometimes within the mortar in which the tie has been embedded. However, conventional Code requirements specify corrosion testing for the whole of the tie material within the cavity space, without recognition of the possibility that localized corrosion may be more significant [11,12]. Whether such Code requirements are meaningful for prediction of long-term corrosion behaviour and capacity requires investigation. It is also unclear at the present time whether the heavy-duty galvanized ties corrode in the same localized manner, whether this applies to stainless steel ties, the effect of mortar type on corrosion and the effect the localized corrosion has on wall tie structural capacity. It follows that as a first step, the actual failure mechanism associated with wall tie corrosion needs to be established and correlated with remaining structural capacity, across the different tie types and for different mortars, irrespective of the actual rate of corrosion that may occur in field situations. The tests described below were aimed at providing insight about these matters.

The next section describes the corrosion and strength tests carried out for conventional and heavy-duty galvanized ties and for stainless steel (SS316) ties in 3 different mortars. One of these (M1) is a typical lime mortar, included for clarification of its effect relative to corrosion of existing and replacement ties in heritage buildings, for which regulatory requirements often mandate lime mortars for repairs and renovation [11]. The other two mortars are typical of those in conventional building practice. Of these M3 is the tie most commonly used in Australia [2,4], while M2 is more economical but somewhat weaker mechanically due to a lower cement to aggregate ratio [11]. A description of the results obtained follows together with analyses of the results. The observations are then discussed in the broader corrosion context of corrosion of embedded materials and the implications that can be drawn from such understanding.

## 2. Materials and methods

### 2.1. Corrosion tests

The overall test program consisted of accelerated corrosion testing using an electrolysis corrosion cell [11,15], and structural tensile testing. For the corrosion testing (Table 1), specimens were constructed in groups of 3 (A, B, C) with 3 different mortar mixes (M1, the lime mortar, M2 and M3) and 3 types of wall tie (R2, R3 and R4) (Figure 2a). The corresponding initial masses for the ties are as shown for each combination (Table 1). The material of each wall tie pair was chosen based on AS3700, Masonry Structures [11], and AS2699, Built-in components for masonry construction [12], and the wall tie exposure classification ratings R2 to R4 (Figure 2b). The chosen materials consisted of (R2) 300 g/m<sup>2</sup> galvanized carbon steel, (R3) 470 g/m<sup>2</sup> galvanized carbon steel, and (R4) 316 L stainless steel. Each material was embedded in M1, M2, and M3 class mortars [11]. The M1 mortar was a heritage mix of lime and sand (i.e., no cement), M2 consisted of a modern lean cement mix, and M3 was a modern cement mortar that is commonly used in present-day construction [7,11]. All mortars were mixed from the same batch: Portland cement (General Purpose), well graded local washed silica beach sand, hydrated plasterer lime, and soft tap water. No additives were used. The mix class volumes of the mortar mixes (Cement: Lime: Sand) were M1 = 0:1:3, with unmeasured water added until a workable condition was reached (visually inferred water binder ratio of 2.0), M2 = 1:2:9, with a

water/cement ratio of 1.90, and M3 = 1:1:6, with a water/cement ratio of 2.0 as per AS3700 [11].

**Table 1.** Corrosion test combinations with initial mass of wall ties for each mortar mix.

Mortar Mix	R2-Conventional Galvanized Steel (~470 g/m <sup>2</sup> )	R3-Heavy duty Galvanized Steel (~950 g/m <sup>2</sup> )	R4-Stainless Steel (Grade 316)
M1 (Lime mortar) 0: 1: 3 <sup>c</sup> w:c = NA <sup>d</sup>	LGM1_A <sup>a</sup> (12.80 g) <sup>b</sup> LGM1_B (12.65 g) LGM1_C (12.56 g)	HGM1_A (19.36 g) HGM1_B (19.58 g) HGM1_C (19.17 g)	SSM1_A (11.22 g) SSM1_B (11.25 g) SSM1_C (11.06 g)
M2 1:2:9 w:c = 1.9	LGM2_A (12.29 g) LGM2_B (12.71 g) LGM2_C (12.52 g)	HGM2_A (20.07 g) HGM2_B (19.66 g) HGM2_C (19.08 g)	SSM2_A (11.25 g) SSM2_B (11.08 g) SSM2_C (11.05 g)
M3 1:1:6 w:c = 2.0	LGM3_A (12.66 g) LGM3_B (12.67 g) LGM3_C (12.72 g)	HGM3_A (19.75 g) HGM3_B (19.52 g) HGM3_C (19.24 g)	SSM3_A (11.08 g) SSM3_B (11.04 g) SSM3_C (11.23 g)

\*Notes: <sup>a</sup>A, B and C represent each of the triplicates.

<sup>b</sup>Initial mass of wall tie.

<sup>c</sup>Mix proportions: volume of cement: volume of lime: volumes of fine sand. The water: cement ratio (w:c) is also shown.

<sup>d</sup>The unmeasured added water was sufficient to make a workable mix (visually inferred w:b = 2.0).

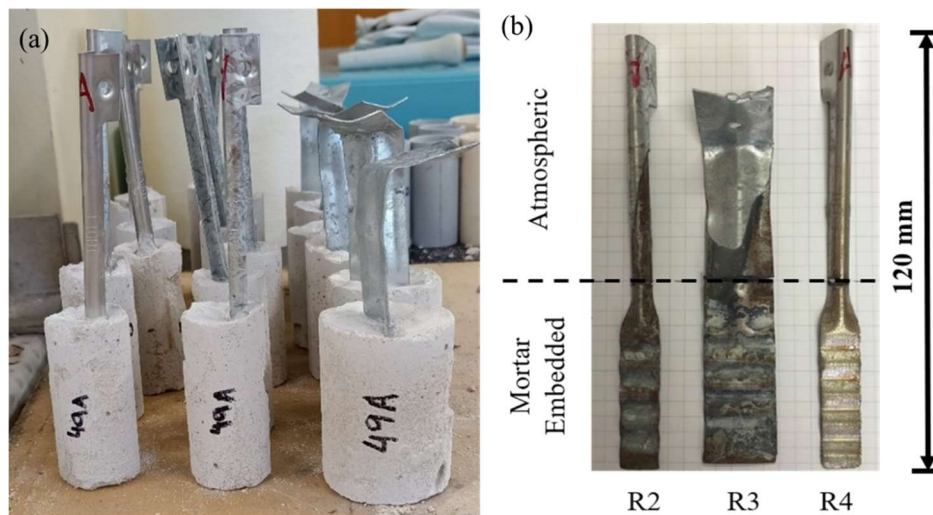


**Figure 2.** (a) Typical mortar-tie specimens prior to exposure, and (b) shapes and dimensions of R2, R3 and R4 wall ties.

The test specimens were constructed as follows. PVC tubes, 70 mm long, 25 mm (R2 and R4) and 40 mm (R3) nominal diameter, fitted with a laminated plywood base fixed with silicon caulk sealant to avoid leakage and to facilitate casting, were used as moulds for the mortar. The length and diameter of the moulds were sufficient to accommodate all types of wall tie tested with sufficient cover all round the corrugated end of the tie (approx 50 mm deep) to closely simulate field conditions. For each specimen, a wall tie was selected at random from those in the sets supplied by the manufacturer, brushed to ensure clean surfaces, and then weighed for initial mass. These were then kept ready for insertion into the relevant mortar mix when completely mixed.

For each mortar mix type sufficient mortar was made for 3 replicates. The mortar was mixed using a Gilson 5QT bench-top laboratory class mixer and placed in the moulds with light tamping. The

relevant ties were then placed in the mortar by hand. Apart from slight wiggling whilst being embedded, the specimens were not subjected to vibration or other compaction techniques. They were allowed to cure for 7 d in the laboratory fog room at room temperature and near 100% relative humidity conditions. All specimens were individually labelled as soon as they were completed.

After curing, the specimens were de-moulded and then subjected to accelerated corrosion testing in an electrolysis cell consistent with ASTM standards [15,16]. The same cell was used for all tests to ensure that, independent of mortar type and tie material combination, all specimens were exposed to identical corrosion conditions [15,16]. The cell consisted of a simple  $300 \times 150 \times 100$  mm deep plastic container, to house the specimen (as anodes), the locally sourced Newcastle beach natural seawater electrolyte and the cathode. The latter was a  $100 \times 100 \times 3$  mm 304 stainless steel plate, with size chosen to match the length of the specimens. The specimens were placed equidistant from the cathode to avoid any change in solution resistivity, which in turn could lead to undesirable current concentrations. Fresh seawater electrolyte was used for each individual specimen corrosion cell so as to avoid changes in solution resistivity caused by the formation of corrosion products. Except for a small area of the wall-tie end fold, which was used for electrical contact, each specimen was completely submerged.

A Tenma Dual DC 0-30 volts regulated power supply set to its maximum 3 A output was used to accelerate corrosion of the specimens. After each specimen had been exposed for 30 min, it was removed from the electrolysis bath, the mortar was carefully chiselled from the wall tie, and this was then wiped clean to allow assessment of the location and the amount of corrosion damage. The cleaned specimens were weighed to estimate overall average corrosion mass loss. To assess whether there was a significant difference between overall corrosion and that of the various parts of each tie, that is, corrosion at the tie-mortar interface region and corrosion in the remaining part of the tie in the cavity, the corroded ties were sheared at the mortar-atmosphere interface and also 10 mm away. This 10 mm section was assigned as being the interface zone. The masses for these corroded segments were then determined. A similar action was performed for uncorroded ties at the same locations to estimate the proportion of each of the original masses and also the proportional surface area for the interface zone and the cavity zone. From this information the corrosion mass losses per unit area were determined for these two zones as well as for the embedded zone.

## 2.2. Structural strength tests

To ascertain the effect of corrosion on tie performance, selections of corroded ties as well as on un-corroded ties were subjected to tensile testing, including load-deformation testing. Two of the triplicate corroded specimens were used. The remaining specimen was used to ensure normalization of the corroded surface area, as explained further below. The tensile tests were performed on an MTS 500 kN universal testing machine.

Because of their non-simple original shape, some preparation was required before the wall tie samples could be tested. For the R2 (conventional) and the R4 (stainless steel) ties (Figure 2), the ends of the ties were flattened over their complete length in order to avoid potentially undesirable stress concentrations at the grips of the testing machine. This was done gently with a hammer taking care not to introduce any excessive plastification of the tie specimens. For the R3 specimens the sharply bent end (Figure 2) was cut off prior to testing. Due to the limited size of the specimen, a conventional extensometer could not be used. To estimate the elongation of the tie materials, reference marks, which

can be seen on Figure 5, were placed on each specimen to measure average strain and thus estimate the average elongation from stress and average strain results.

### 3. Results

#### 3.1. Corrosion losses

For the overall results for corrosion mass loss, the individual readings were averaged for each tie type and then divided by the relevant surface (i.e., exposure) area. The latter are summarized in Table 2. The results for overall mass loss of the ties (in  $\text{mg}/\text{mm}^2$ ), the mass loss for the embedded zones of ties (i.e., that part of the tie embedded in the mortar) and the part of the tie considered as in the interface zone immediately adjacent to the mortar are shown in Table 3. The interface zone was assigned as the surface area in a patch 10 mm long around the circumference of the wall tie, immediately adjacent to the mortar surface. An overview of the condition of the wall ties after corrosion is shown in Figure 3. There is not much difference between the visual appearances of the ties except that type R4 (stainless steel) shows very little overall corrosion.

**Table 2.** Exposure areas for wall ties.

Tie type and mortar	Approximate overall size (mm)	Total surface area ( $\text{mm}^2$ )	Surface area embedded in mortar ( $\text{mm}^2$ )	Surface area for Interface zone ( $\text{mm}^2$ )	Surface area for cavity zone ( $\text{mm}^2$ )
R2 (M1–M3)	$143 \times 11 \times 3$	1796	660	110	1026
R3 in M1	$138 \times 23 \times 7$	3161	1380	234	1546
R3 in M2	$138 \times 23 \times 7$	3161	1380	250	1531
R3 in M3	$138 \times 23 \times 7$	3161	1380	271	1509
R4 (M1–M3)	$143 \times 11 \times 3$	1796	660	110	1026

**Table 3.** Corrosion mass losses for ties in overall exposure and for the mortar embedded, interface and net cavity zones.

Mortar type	Tie type	Overall ( $\text{mg}/\text{mm}^2$ )	Mortar embedded ( $\text{mg}/\text{mm}^2$ )	Interface ( $\text{mg}/\text{mm}^2$ )	Net cavity ( $\text{mg}/\text{mm}^2$ )
M1	R2	0.95	0.93	0.022	0.497
	R3	2.09	0.86	1.235	0.043
	R4	0.97	0.85	0.116	0.757
M2	R2	0.86	0.27	0.580	0.741
	R3	1.23	0.28	0.945	0.329
	R4	1.13	0.16	0.966	1.009
M3	R2	2.77	0.28	2.490	0.898
	R3	2.09	0.46	1.631	0.573
	R4	1.00	0.02	0.981	0.922

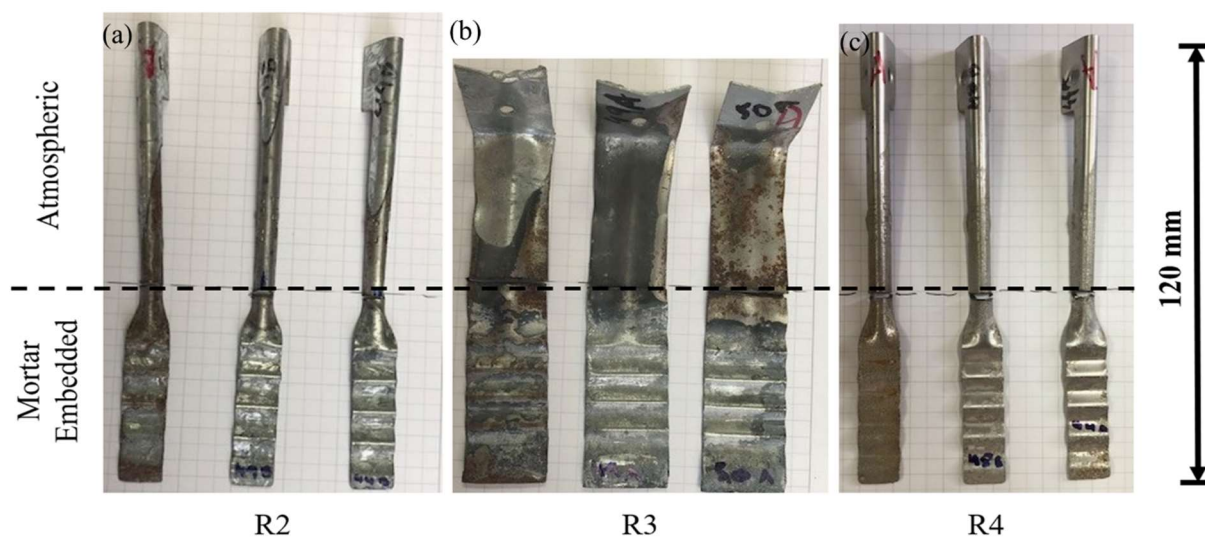


**Figure 3.** Overview of the relative condition of ties (a) R2, (b) R3 and (c) R4 in each case after exposure for embedment in (a to c) mortar type M1, mortar type M2 and mortar type M3.

Close observation of the surfaces of ties did show corrosion damage in the form of localized corrosion (Figure 4). This is particularly so for the localized corrosion in the interface zone of the stainless-steel ties (R4) even though overall corrosion is relatively low compared to that for the R2 and R3 ties (Table 3). A similar effect for R4 ties is seen for the type M2 mortar (Table 3) that has a lower proportion of cement (Table 1).

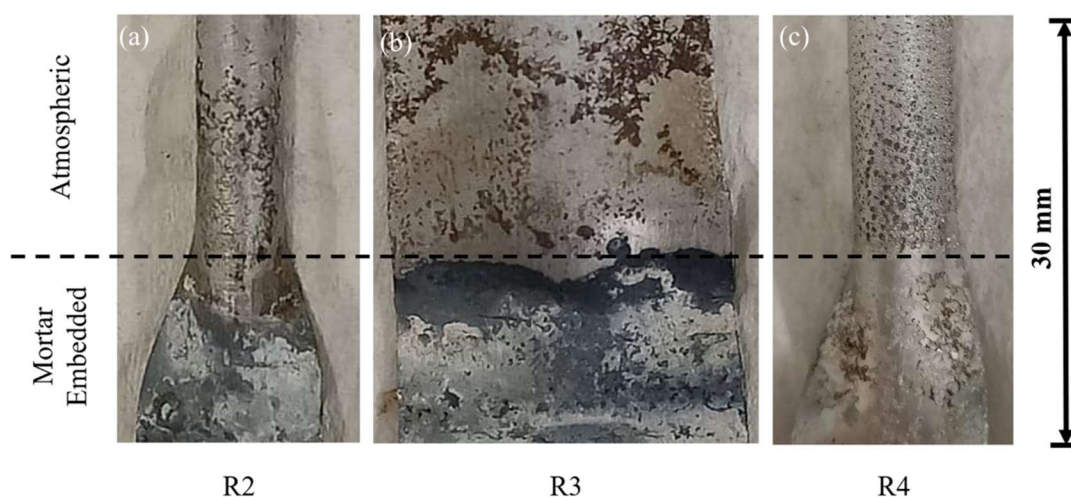


**Figure 4.** (a) Close-up views of corrosion damage of ties in the interface zone, (b) for ties R2, R3 (c) R4, in each case embedded in M3 mortar.

### 3.2. Structural capacity effects

The results of the tensile testing of the ties are shown in Table 4. For each tie type the first 3 lines refers to the tie properties for unexposed specimens, selected at random from those supplied for the test program. The values that follow in subsequent rows show the values for the corroded mortar embedded specimens. The observed failure modes for each of the specimens tested in tension are shown in Figure 5.

**Table 4.** Proof stress, ultimate tensile strength, elongation and observed failure zone location in tensile tests (average of two test results).

Mortar type	Tie type	Stress at 0.2% yield (n/mm <sup>2</sup> )	Ultimate tensile strength (n/mm <sup>2</sup> )	Elongation (%)	Failure zone
Unexposed, Bare Controls	R2	268	494	5.0	G
	R3	284	768	12.0	C
	R4	358	849	17.0	C
M1	R2	279	408	5.0	M
	R3	273	740	13.0	G/I
	R4	381	613	10.0	M/C
M2	R2	231	358	5.0	I/C
	R3	167	690	10.0	C
	R4	264	327	2.0	C
M3	R2	151	333	4.0	I/C
	R3	225	671	12.0	G/I
	R4	289	593	7.0	I

\*Notes: Failure zone locations:

G = failure at or apparently having initiated from tensile test grip of the tensile testing machine.

C = within the cavity between brick leaves or between brick leaf and plasterboard.

M = within the mortar embedded zone.

I = at or within 10 mm of the inner face of the masonry leaf, i.e., at the tie-brick interface.



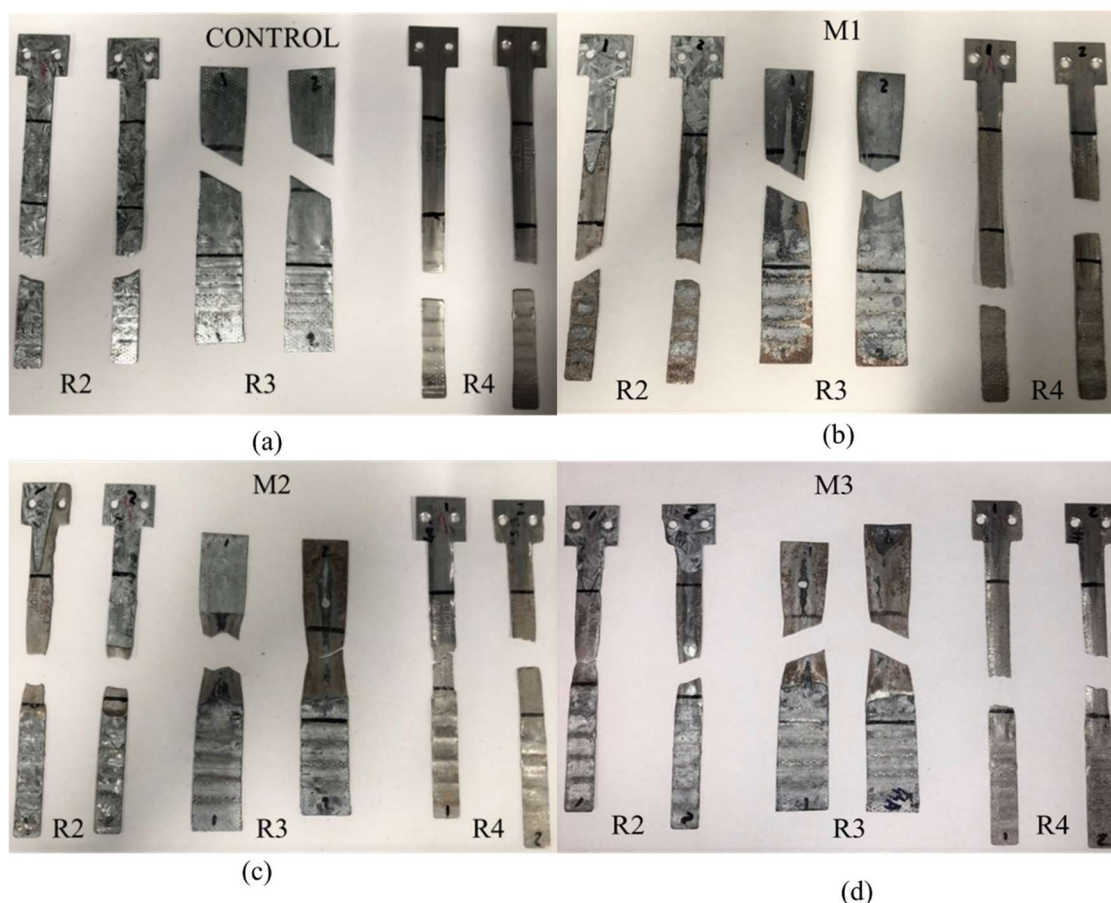


**Figure 5.** Failure modes of tie specimens R2, R3 and R4 tested in tension: unexposed control ties (a), and exposed ties after removal of the lower end from mortars M1 (b), M2 (c) and M3 (d). The black lines define the ends of the grips of the tensile testing machine.

Considering first the results for the strength testing, it is seen from Table 4 that, overall, the net capacity in tension of ties embedded in mortar is less than the original unexposed capacity of the tie. This is to be expected because of the effect on cross-sectional area of corrosion but also owing to the strength of the mortars and the need to transfer the tensile force in the tie through shear and some degree of mechanical interlock to the body of the mortar. Thus, ties of grade R2 showed quite modest loss of overall capacity as measured by ultimate tensile strength (UTS) for all three mortars, with somewhat greater loss of proof strength but with reference to the unexposed ties, some loss of elongation capacity at proof stress for the two cement-based mortars (M2 and M3). Ties of grade R3 showed a generally similar pattern although with greater relative loss of proof strength and of UTS for the cement mortars M2 and M3, while there was only a slight reduction of elongation when embedded in M1 and M2 and somewhat more in M3.

At first sight the relatively large drop in UTS and elongation at proof strength of the R4 (stainless steel) ties might seem surprising given that the loss in proof strength (0.1% stress), while significant, is, relatively, more modest. The loss in UTS and elongation could be the result of material embrittlement (i.e., loss of ductility) due to intergranular stress corrosion cracking, which has been extensively reported for austenitic stainless steels (i.e., 316 SS) within chloride-rich aqueous environments, most of which are underpinned by classic Cragnolino and McDonold work [17]. It is

noteworthy, as per Table 3 results, that while the R4 316 SS ties showed a lower mass loss compared to the R2 and R3 classes, their relative capacity loss of these ties was significantly higher. This can be attributed to more severe localized corrosion on the R4 ties in the interface region (Figure 4).

The overall, mortar embedded, interface and net cavity corrosion zones (Table 3) show quite differences in intensity of corrosion. Compared to the two cement mortars (M2 and M3) corrosion loss of all ties was relatively compared to that in the M1 (lime) mortar (Table 3). And this corresponds with the location of the failure mode for the ties tested in tension (Table 5). For the most commonly used mortar (M2) failure tended to be in the cavity zone even though the corrosion losses were relatively less than those for the weaker M3 mortar were mainly in the interface zone, corresponding to higher corrosion losses in that zone (Table 5). It should be clear that the ultimate tensile strength observed in the tests is governed by the weakest zone, as can be seen by comparing the corrosion and failure zones in Table 5 with the recorded UTS values.

**Table 5.** Correlation between corrosion in various zones of tie exposure and UTS (Ultimate Tensile Stress) of ties and with visual observations of failure mode.

Mortar type	Tie type	Mortar embedded (mg/mm <sup>2</sup> )	Interface (mg/mm <sup>2</sup> )	Net cavity (mg/mm <sup>2</sup> )	Ultimate Tensile Stress (N/mm <sup>2</sup> )	Visual failure mode
M1	R2	<b>0.93</b>	0.022	0.497	408	<b>M</b>
	R3	0.86	<b>1.235</b>	0.043	740	<b>G/I</b>
	R4	<b>0.85</b>	0.116	0.757	613	<b>M/C</b>
M2	R2	0.27	<b>0.580</b>	<b>0.741</b>	358	<b>I/C</b>
	R3	0.28	<b>0.945</b>	0.329	690	<b>C</b>
	R4	0.16	0.966	<b>1.009</b>	327	<b>C</b>
M3	R2	0.28	<b>2.490</b>	0.898	333	<b>I</b>
	R3	0.46	<b>1.631</b>	0.573	671	<b>G/I</b>
	R4	0.02	<b>0.981</b>	0.922	593	<b>I</b>

\*Notes: Bold figures match visual observations of failure in tension

G = near tensile test grip of testing machine.

C = within the cavity.

M = within the mortar embedded zone.

I = at or very near the tie-brick interface.

#### 4. Discussion

There are various observations in the literature that relate to the above experimental observations and can assist in placing them in context. Most relevant should be observations for steel reinforcement in concrete [18], for galvanized steel in concrete [19] and for stainless steel reinforcement [17,20] as well as observations from practical experience. These experiences indicate that heavy duty galvanizing can be protective to the steel through its galvanic cathodic protective effect [21], and that stainless steels tend to have a greater long-term resistance to corrosion through the presence of a chromium oxide surface film, but only when there is sufficient access of oxygen to repair any damage to that film [20,21]. The alkalinity of the concrete or mortar surrounding the steel tends to inhibit corrosion initiation and this can be expected also for cementitious mortars [19]. All these observations refer to continuous surfaces or interfaces. However, it is well-known that at junctions of metals with other

metals or other materials there can be highly localized corrosion in the form of pitting or crevice corrosion, irrespective of whatever corrosion protection or inhibition occurs further away [21]. Such localized effects can be seen in the wall tie-mortar specimens considered herein. This was the case for higher cement content mortar M3 (i.e., highest relative cement content), even with stainless steel ties where failure in tension occurred at the interface region (Table 5). Figure 4 shows such localized corrosion at the interface regions for the two classes of galvanized ties (R2, R3) and also for the stainless-steel tie (R4). Possible corrosion mechanisms to provide the localized corrosion of the ties at the interface region are shown schematically in Figure 6a for mortars with very low or zero cement content (e.g., lime mortars) and Figure 6b mortars with high cement content (e.g., cementitious mortars).

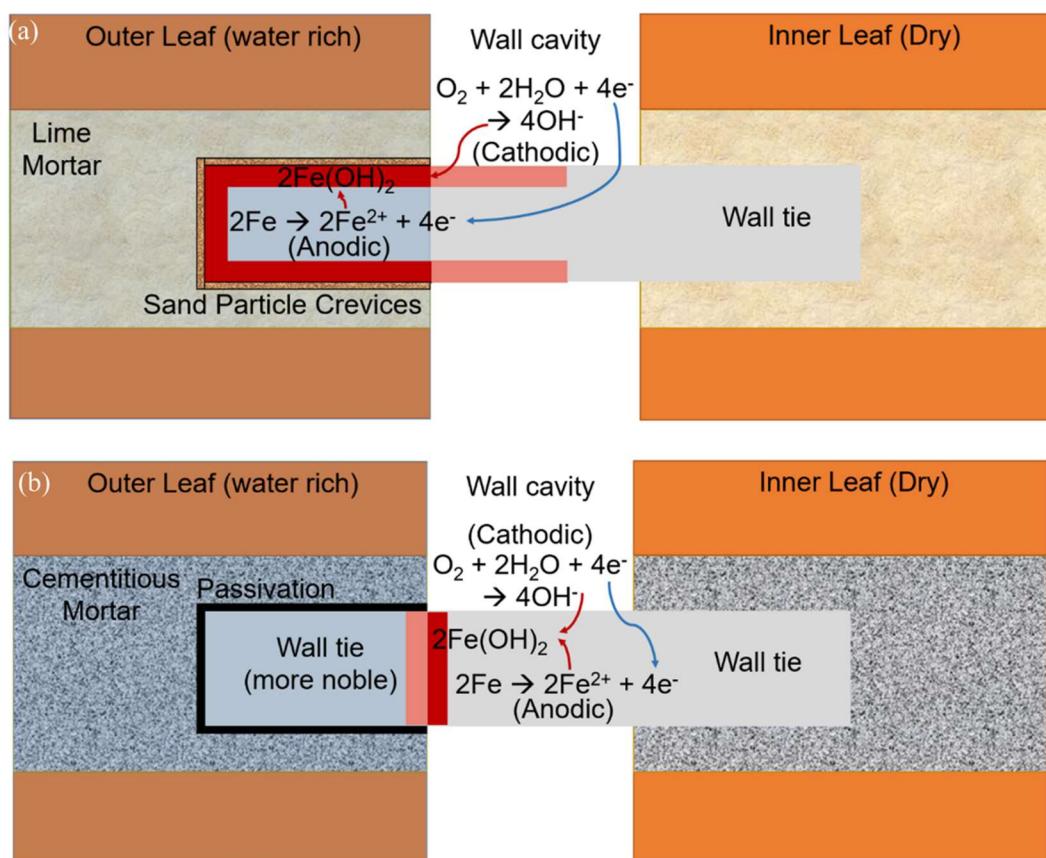


**Figure 6.** Schematic of corrosion kinetics for mortar embedded brick veneer and cavity brick metal wall ties where (a) mortar cement content is low (i.e., lime mortars) and (b) cementitious mortars.

In terms of practical implications of the above findings, it is clear that localized corrosion plays a critical role in the relationship between corrosion and the structural capacity of ties, more so than atmospheric corrosion in the cavity or corrosion in the embedded zone (Table 5). These findings might be compared to the current recommendations for the selection of brick ties [11,12]. These are based on the R rating which in turn is based on resistance to general corrosion, for example as estimated in a salt spray chamber, or by electrochemical tests. As is well-known, such tests being unable to make sound estimates of resistance to localized corrosion, and this is demonstrated also by the results in

Table 5. If strength of the ties is the main criterion for effectiveness in applications, as is usually considered the case, their capacity in tension (or compression) is important, and as shown herein, such strength may be governed by localized corrosion. Hence the standard classification system and the tests on which it is based may be quite misleading. In particular, the above results suggest that the current practice of recommending stainless steel ties may be misleading for application in aggressive marine exposure conditions.

It is important to note that the observations and conclusions presented herein are based on relatively short-term exposure periods and are for under artificially accelerated conditions. The extent to which they apply to wall tie corrosion and strength behaviour under longer-term field conditions is an issue that is similar to, and that has parallel issues with, the need for extending observations for reinforced concrete [2,4–6,14]. In this context a potential difficulty for verification of such extensions is the fact that there are only a few reports about long-term behaviour of wall ties, including corroded wall ties [4]. This extends also to structural capacity estimations. It follows that there is scope for future empirical parametric studies to develop better understanding of these matters. It also follows that there are likely to be continued amendments to design standards and to design considerations for new unreinforced masonry veneer and cavity wall infrastructure.

## 5. Conclusions

The following conclusions are drawn from the material presented herein:

- (1) For the most commonly-used modern cement mortar (M3), under identical electrolytic corrosive conditions R2 light galvanized steel ties presented higher overall mass loss (about 40% greater) relative to R3 heavy galvanized steel ties, with R4 grade 316 stainless steel ties presenting the lowest level of overall mass loss (about 50%). This is consistent with their classification for modern construction.
- (2) The increased alkalinity from cementitious mortars inhibits corrosion initiation at the embedded portion of the wall tie, which, by becoming cathodic (more noble) in relation to its adjacent atmosphere (cavity) interface, leads to a localized corrosion effect at mortar cavity interface.
- (3) Stainless steel R4 class ties presented significantly greater relative losses of yield strength, ultimate tensile strength and elongation structural capacity compared to R2 low galvanized and R3 heavy galvanized tie classes. This is due to their known greater susceptibility to highly localized corrosion at the mortar cavity interface.
- (4) There should be some concern about the appropriateness of the current standard classification practice that recommends stainless steel wall ties for application in aggressive marine exposure conditions. As shown herein, for stainless steel wall ties, capacity in tension (or compression) can be seriously affected by localized corrosion.

## Acknowledgments

Technical assistance provided by The University of Newcastle's Civil, Surveying and Environmental Engineering Laboratory Staff is greatly appreciated. This research was funded by The Summer Scholarship Scheme of The University of Newcastle's Faculty of Engineering and Built Environment.

## Conflict of interest

The authors declare no conflict of interest.

## References

1. Lawson RM, Popo-Ola SO, Way A, et al. (2009) Durability of light steel framing in residential applications. *P I Civil Eng-Munic* 163: 109–121. <https://doi.org/10.1680/coma.2010.163.2.109>
2. Jardim do Nascimento B, Chaves IA, Masia MJ, et al. (2017) A field investigation into long-term corrosion of metal wall ties in masonry veneer construction, *Proceedings of the 10th Australasian Masonry Conference*, Sydney: The University of Newcastle, 1–12.
3. Brick Industry Association (2003) *Wall Ties for Brick Masonry*. Reston: Brick Industry Association, 1–15.
4. Chaves IA, De Prazer S, Jardim do Nascimento B, et al. (2021) Empirical coastal atmospheric corrosion of masonry metal wall ties. *J Corr Mater Degrad* 2: 657–665. <https://doi.org/10.3390/cmd2040035>
5. Page AW, Kleeman PW, Stewart MG, et al. (1990) Structural aspects of the Newcastle earthquake. *2<sup>nd</sup> National Structural Engineering Conference*, Adelaide: Institution of Engineers.
6. Page CL (1985) Barriers to the prediction of service life of metallic materials, In: Masters LW, *Problems in service life prediction of building and construction materials*, Netherlands: Springer.
7. Urban Development Institute of Australia–Western Australia, Modern Methods of Housing Construction, 2020. Available from: <https://www.udiawa.com.au/wp-content/uploads/2021/01/FINAL-UDIA-Report-Modern-Methods-of-Construction.pdf>.
8. National Recovery and Resilience Agency, Australian Government, Building codes are not enough to protect homes against water damage in severe storms, 2017. Available from: <https://knowledge.aidr.org.au/resources/research-building-codes-are-not-enough-to-protect-homes-against-water-damage-in-severe-storms>.
9. Department of Fire & Emergency Services, Government of Western Australia, Storm safety information, 2021. Available from: <https://www.dfes.wa.gov.au/safetyinformation/storm>.
10. Ginger J, Henderson D, Edwards M, et al. (2010) Housing damage in windstorms and mitigation for Australia. *James Cook University Research Report*: 1–18. Available from: [https://researchonline.jcu.edu.au/16337/1/Ginger\\_IGWRDRR\\_Aust\\_Final.pdf](https://researchonline.jcu.edu.au/16337/1/Ginger_IGWRDRR_Aust_Final.pdf).
11. Standards Association of Australian (2018) *AS 3700 Masonry Structures*, Sydney: Standards Australia.
12. Standards Association of Australian (1998) *AS 3826 Strengthening Existing Buildings for Earthquake*, Sydney: Standards Australia.
13. Jardim do Nascimento B, Chaves IA, Masia MJ, et al. (2019) Corrosion behaviour of mortar embedded wall-ties in natural and artificial environments, *Australasian Corrosion Association Annual Conference*, Melbourne: Proceedings of the Corrosion & Prevention, 24–17.
14. Hagel MD, Liesel SL, Sturgeon GR (2007) Comparison of theoretical and empirically determined service lives for wall ties in brick veneer steel stud wall systems. *J Civ Eng* 34: 1424–1432. <https://doi.org/10.1139/L07-018>
15. ASTM International (2019) Standard guide for conducting and evaluating Galvanic corrosion tests in electrolytes, ASTM G71-81.

16. ASTM International (2011) Standard practice for preparing, cleaning and evaluating corrosion test specimens, ASTM G1-03.
17. Cragolino G, McDonald DD (1982) Intergranular stress corrosion cracking of austenitic stainless steel at temperatures below 100 C–A review. *Corrosion NACE* 38: 406–424. <https://doi.org/10.5006/1.3577354>
18. Melchers RE, Chaves IA (2018) Service life estimation of concrete infrastructures. In: Fernando Pacheco-Torgal, Robert Melchers, Nele de Belie, *Eco-efficient Repair and Rehabilitation of Concrete Infrastructures*, England: Woodhead, 13–37.
19. Raupach M (2007) *Corrosion of Reinforcement in Concrete: Mechanisms, Monitoring, Inhibitors and Rehabilitation Techniques*, England: Woodhead.
20. Lidija MS, Valek-Žuljb V, Bjegovića D (2013) Long-term corrosion behaviour of stainless reinforcing steel in mortar exposed to chloride environment. *J Corr Sci* 69: 149–157. <https://doi.org/10.1016/j.corsci.2012.11.035>
21. Evans UR (1948) *Metallic Corrosion Passivity and Protection*, London: Edward Arnold.



AIMS Press

© 2022 the Author(s), licensee AIMS Press. This is an open access article distributed under the terms of the Creative Commons Attribution License (<http://creativecommons.org/licenses/by/4.0>)